Langmuir

Article

pubs.acs.org/Langmuir

Smooth, Aggregate-Free Self-Assembled Monolayer Deposition of Silane Coupling Agents on Silicon Dioxide

Roger M. Diebold*[,†,‡] and David R. Clarke[†]

[†]School of Engineering and Applied Sciences, Harvard University, Cambridge, Massachusetts 02138, United States

[‡]Materials Department, University of California, Santa Barbara, Santa Barbara, California 93106, United States

Supporting Information

ABSTRACT: Silane coupling agents (SCAs) are notorious for aggregating during deposition on oxide substrates, leading to nonuniform surface morphologies. To ameliorate this problem, we describe a vapor-phase deposition technique for silane coupling agents employing a spin-coated perfluoropolyether (PFPE) diffusion barrier that facilitates the formation of smooth, aggregate-free self-assembled monolayers (SAMs). Samples fabricated using PFPE barrier layers yielded SAMs exhibiting similar water contact angles, reduced water contact angle hysteresis, and a 2-fold reduction in rms roughness relative to those without a barrier. X-ray photoelectron spectroscopy confirms that the barrier layer can be completely removed after deposition, leaving behind a smooth monolayer. A basic analysis of the agglomerate separation ability of the barrier layers is discussed to understand the critical parameters involved. Generalized guidelines for selecting barrier materials are presented.

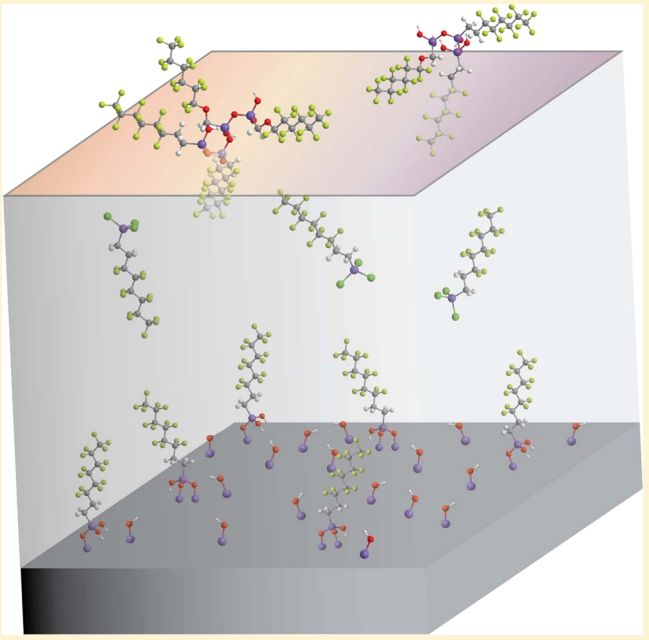

INTRODUCTION

Silane coupling agents (SCAs) have been employed in industry and academia for decades in a variety of applications: to enhance bonding between fillers and polymer matrices,[1] improve particle dispersion in a polymer matrix,[2] and act as antistiction layers for microelectromechanical systems.[3,4] Although the widespread use of SCAs is a testament to their versatility and utility, the tendency for these molecules to aggregate and form rough surfaces can be problematic for applications that are disrupted by inhomogeneous surface morphologies. For example, the electrically insulative properties of self-assembled monolayers (SAMs) are strongly dependent on disorder[5] and defects that can arise around the edge of agglomerates;[6] a typical SCA deposition on oxide will result in multilayers and agglomerates strongly bound to the surface. Although there are a multitude of commercially available chemistries, each SCA exhibits a different tendency to form agglomerates, typically dictated by the reactivity of the hydrolyzable binding groups and steric properties of the molecule. Thus, a direct comparison of different SCA chemistries on an oxide surface is often frustrating largely because it is difficult to decouple morphology from chemistry. Additionally, researchers investigating phenomena that require homogeneous morphologies typically shun SCA/oxide systems in favor of alkanethiol/gold systems as smooth monolayers are more readily and reproducibly formed.[7] In this article, a simple method for producing smooth, aggregate-free monolayers of vapor-deposited SCAs on silicon dioxide is demonstrated using a perfluoropolyether (PFPE) barrier layer.

In the vapor phase, there are four routes to reducing SCA agglomeration on an oxide surface: creating a dry environment for deposition, reducing deposition time, reducing the deposition temperature, and using monofunctional SCA molecules. A truly dry medium for SCA deposition, either liquid or gaseous in nature, is extremely difficult to achieve in practice and may be available only under ultrahigh vacuum conditions. Because the SCA molecules require at most only a few molecules of water to hydrolyze, it is impractical to prevent premature reaction completely. It is also useful to note that depositing SCAs in the liquid phase has been shown to produce

Received: July 7, 2012
Revised: October 11, 2012

   dx.doi.org/10.1021/la303377w | *Langmuir* XXXX, XXX, XXX−XXX

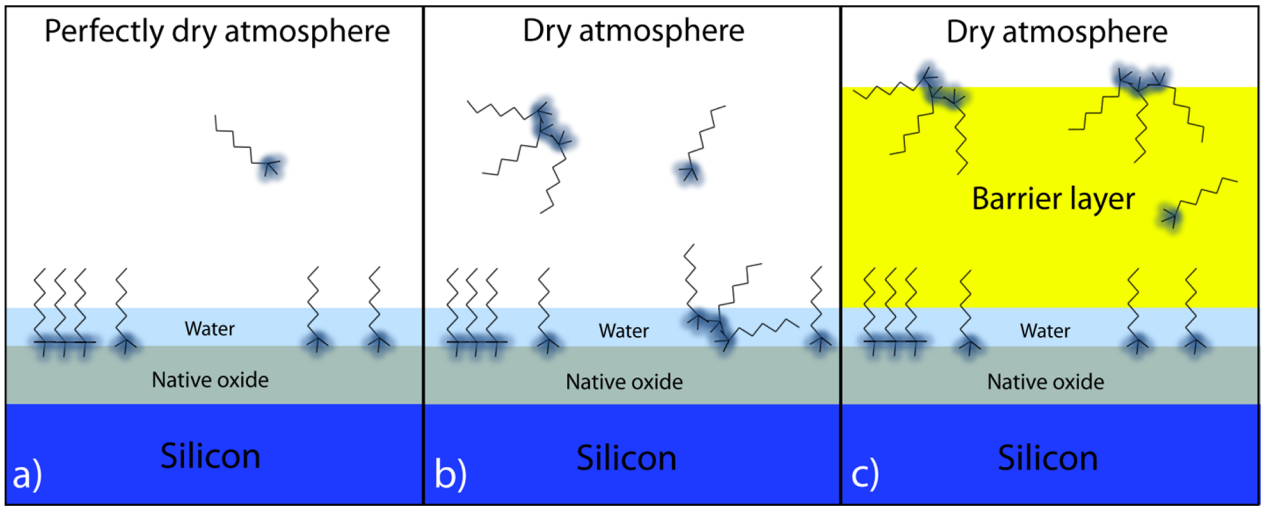

Figure 1. (a) Schematic of an idealized vapor deposition process. (b) Realistic vapor deposition in which agglomeration occurs before binding to the surface. (c) Realistic vapor deposition with an oil barrier layer showing agglomerates diffusing slowly through the barrier layer relative to individual SCA molecules. An example of a trifunctional SCA molecule is depicted, with the binding groups highlighted in blue and the R group shown as a linear alkane chain. For di- or trifunctional SCAs, cross-linking in the plane is expected depending on molecular proximity,[15] which is a function of the SCA surface concentration and surface hydroxyl concentration.

rougher SAMs than in the vapor phase.[8] Reducing the deposition time reduces the SCA concentration on the target surface, which in many cases is unsatisfactory because dense monolayers are typically desired. Reducing the deposition temperature has been observed to reduce defects within SCA SAMs in solution,[7] and although the reaction kinetics at the surface are slowed, this does not necessarily imply that longer deposition times are required.[9] Rather, in the vapor phase, deposition will proceed more slowly, specifically because lower temperatures will lower the SCA vapor pressure. Monofunctional SCAs not only restrict the functionalizing chemistries that can be chosen, but the molecules inherently lack hydrolytic and thermal stability relative to those with trifunctional binding moieties.[4] As an alternative, it has been suggested by Benkoski et al. that triacylglycerols or naturally occurring carbon can act as barriers for SCA agglomerates under solution deposition conditions.[10] A spin-coated and washed triacylglycerol layer applied to a silicon dioxide surface before (3-glycidoxypropyl)-trimethoxysilane deposition resulted in SAMs that yielded similar water contact angles to that of a "smooth" monolayer, produced from an as-received silicon dioxide substrate coated with a barrier layer composed of naturally occurring carbon. The same authors attempted to use hexadecane as another type of barrier layer, but this resulted in rough morphologies likely because the washing procedure removed most of the hexadecane before SCA deposition commenced. The authors discussed the experiments in order to understand further the effects of the naturally occurring carbon layer on the resulting SAM morphology but did not pursue this barrier concept further.

In exploring this barrier concept with PFPE on silicon dioxide, it is found that SCA agglomerates can be prevented from forming. High advancing water contact angles are maintained with reduced SAM roughness and water contact angle hysteresis. X-ray photoelectron spectroscopy (XPS) measurements confirm that the washing method described herein removes all residual PFPE regardless of the initial quantity, leaving behind a smooth SCA monolayer. The limits of this technique are investigated in order to obtain smooth, aggregate-free, dense SAMs of SCAs on silicon dioxide and other substrates.

To place our work in context, SCAs binding to a silicon dioxide surface is typically idealized as follows (Figure 1). SCA molecules diffuse from their source to the oxide surface where they encounter physisorbed water bound to surface hydroxyls. After hydrogen bonding to the surface water, the SCA binding groups are hydrolyzed, converting them into SCA silanols that condense with the surface hydroxyl groups, creating covalent siloxane linkages from the SCA to the oxide. In principle, the process is self-limiting in that each SCA molecule bonds only to surface silanols or neighboring SCA molecules such that the R group is oriented perpendicular to the surface and a single dense monolayer is formed. This depiction is unrealistic in that amorphous oxide surfaces contain a spatially random distribution of hydroxyl sites influenced by local curvature,[11] to which only one or two SCA silanols may bind because of steric hindrance.[12] As each SCA self-organizes at a specific angle to the surface normal depending on the temperature, local hydroxyl concentration, and steric considerations, disorder is typically observed in SAMs on oxide.[13] Consequently, SCA molecules on fully hydroxylated silicon dioxide typically exhibit an average tilt normal to the surface whose self-assembly has been verified by Genzer et al. using near-edge X-ray absorption fine structure measurements.[14] If there is excess water present in the deposition medium (i.e., atmosphere) beyond the minimum necessary to allow bonding to the substrate, SCA molecules are likely to hydrolyze prematurely and bind to other SCA molecules forming agglomerates,[7−9] which can settle and adhere to the sample surface. Another nonideality is the nonequilibrium concentration of water at the surface during deposition. The oxide samples are usually exposed to piranha or similar oxidative cleaning processes immediately before SCA deposition to fully hydroxylate the surface and remove organic contaminants. This ensures that the surface is hydrophilic and promotes the presence of multiple molecular layers of water.[11] When the sample is then inserted into the SCA deposition chamber, the dry atmosphere promotes water evaporation and thus changes the concentration of water at the sample surface

dx.doi.org/10.1021/la303377w | *Langmuir* XXXX, XXX, XXX−XXX

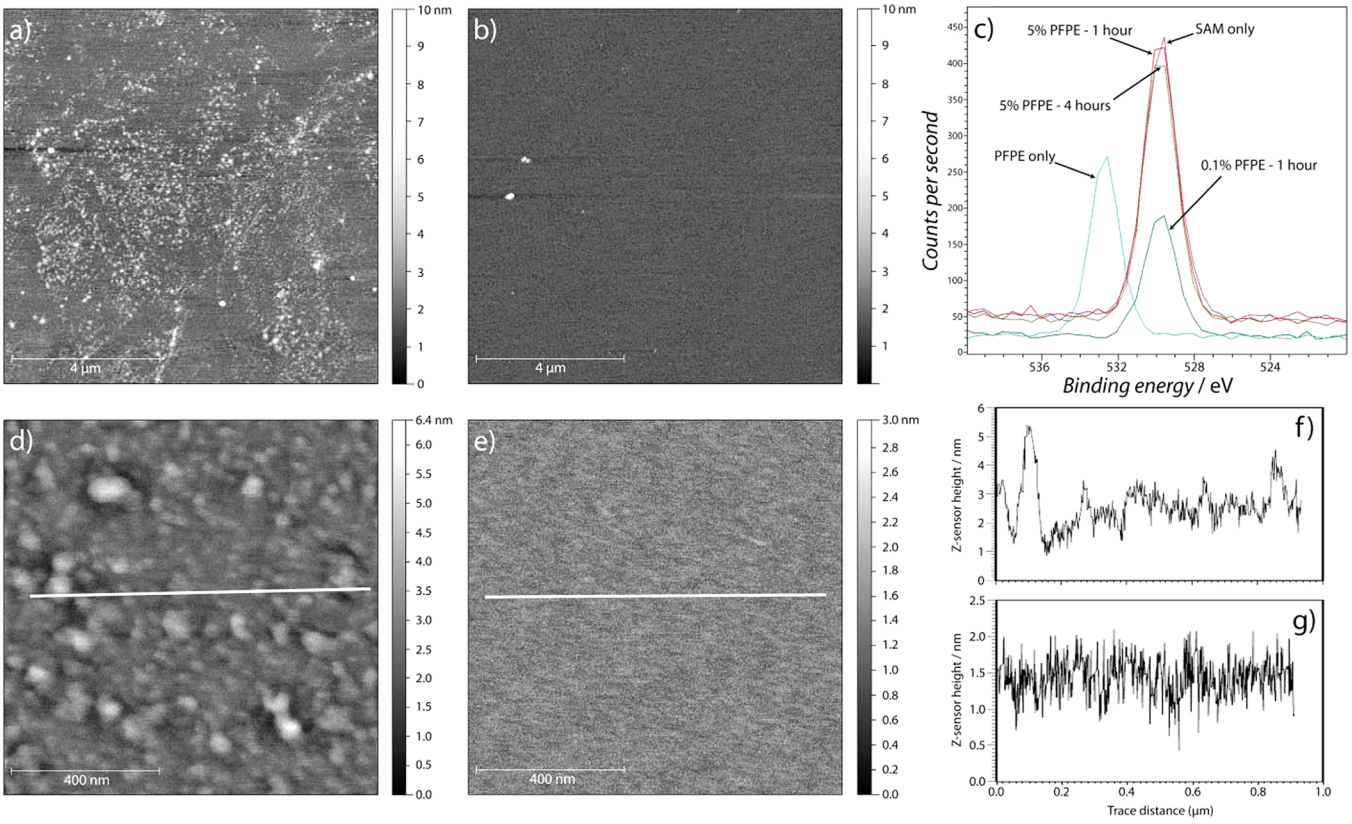

Figure 2. Representative tapping mode z-sensor AFM images of SAMs on (a) bare oxide, unheated prior to 4 h of SCA deposition and (b) 5% PFPE solution spin coated on oxide, unheated prior to 4 h SCA deposition. (c) XPS O 1s peaks for representative samples and controls. It is evident that no PFPE remains after washing because the peak positions of the mixed PFPE/SCA samples closely match those of the SAM-only sample because they are separated from the PFPE-only peak by ∼3 eV. The data labels refer to the percent PFPE solution and the SCA deposition time (in hours). The SAM-only sample was deposited for 4 h without heating prior to PFPE application, and the PFPE-only sample was cast from a 5% solution without prior heating. The PFPE/SCA samples were all heated prior to oil deposition. All survey scans were calibrated by their largest peak (F 1s), which was set to 686 eV prior to comparison between the spectra. Close-up 1 μm × 1 μm tapping-mode AFM images in a and b are shown in d and e, respectively. Linear profile traces exhibited by white lines in d and e are given in f and g.

as a function of time. Although this is a secondary benefit relative to requiring agglomerate diffusion through a viscous layer, the change in water concentration over time may lead to irreproducible SAMs.[7] This may also mitigate issues with SAM quality between depositions if variations in atmospheric humidity are experienced (e.g., improper purging).

EXPERIMENTAL SECTION

A 100-mm-diameter Sb-doped silicon wafer (0.005−0.0018 Ω·cm, prime grade, University Wafer, Inc.) was cleaned in Nanostrip (Cyantek, Co.), and the native oxide was stripped with hydrofluoric acid (J. T. Baker, Co., 49%). The wafer was left to oxidize naturally under clean-room conditions. After spin coating with a protective layer of photoresist and dicing into 8 mm squares, the wafer was immersed in acetone for 20 min, followed by an isopropanol and deionized (DI) water rinse and then dried with nitrogen. The silicon substrate was further cleaned in Nanostrip (95 °C, 7.5 h) to ensure that all photoresist was removed and the surface was fully hydroxylated, rinsed in DI water, and blow dried with nitrogen. Oxide thicknesses were recorded by ellipsometry (WVASE32, J. A. Woollam, Inc.); 10 different areas of the wafer were measured (average thickness 1.7802 nm, standard deviation 0.012 nm) after partial dehydration (>10 min, 115 °C) to minimize the effect of the adsorbed water layer on thickness. Immediately before deposition, the substrates were treated with room-temperature Nanostrip for 15 s to ensure decontamination and hydroxylate the surface and then heated on a hot plate at 115 °C (sample depending). This was followed by spin coating PFPE (Fomblin Y, 3.3 kDa, LVAC 25/6, Sigma-Aldrich, Inc.) in perfluorooctane (Sigma-Aldrich, Inc., 98%) or silicone oil (Dow Corning Fluid 200, 50 cSt) in heptane (Sigma-Aldrich, Inc., 99%) and vapor depositing the SCA ((tridecafluoro-1,1,2,2-tetrahydrooctyl)-trichlorosilanes, Gelest, Inc., >95%). Control samples without any PFPE barrier were prepared in the same way.

The PFPE, perfluorooctane, heptane, silicone oil, and fresh SCA were filtered prior to deposition through 0.2 μm poly-(tetrafluoroethylene) (PTFE) membranes. Deposition took place at room temperature in a 1 L PTFE jar (Cole-Parmer, Inc.) using double-sided permanent tape (3M Co.) to affix the samples to the center of the jar lid. A clean glass vial (VWR, Inc., 1.1 mL) containing SCA (0.2 mL) was placed within a polystyrene insert in the center of the bottom of the jar. Subsequently, the jar was purged for 30 s with dry argon and closed tightly. After deposition, the samples were ultrasonicated in perfluorooctane for 30 min, rinsed in progressively more polar solvents, and blow dried with air. Samples prepared with silicone oil were washed with xylenes and progressively more polar solvents before drying. To desorb residual SCA molecules and condense dangling SCA hydroxyl groups, all samples were heated for 10 min at 115 °C and vacuum sealed in dry argon.

To characterize the materials, spectroscopic ellipsometry scans were conducted from 500 to 1000 nm at 55, 65, and 75° relative to the sample normal. SAM thicknesses were fit using a 1.7802 nm fixed oxide thickness below a Cauchy layer (initial guess 2 nm) with a refractive index of 1.3521 corresponding to the bulk value of the SCA refractive index. An atomic force microscope (AFM) (MFP-3D, Asylum Research) was employed to evaluate the surface roughness with fresh Si cantilevers (PointProbePlus NCHR, nominal tip radius <10 nm, NanoAndMore, Inc.). Tapping mode AFM scans were taken

dx.doi.org/10.1021/la303377w | Langmuir XXXX, XXX, XXX−XXX

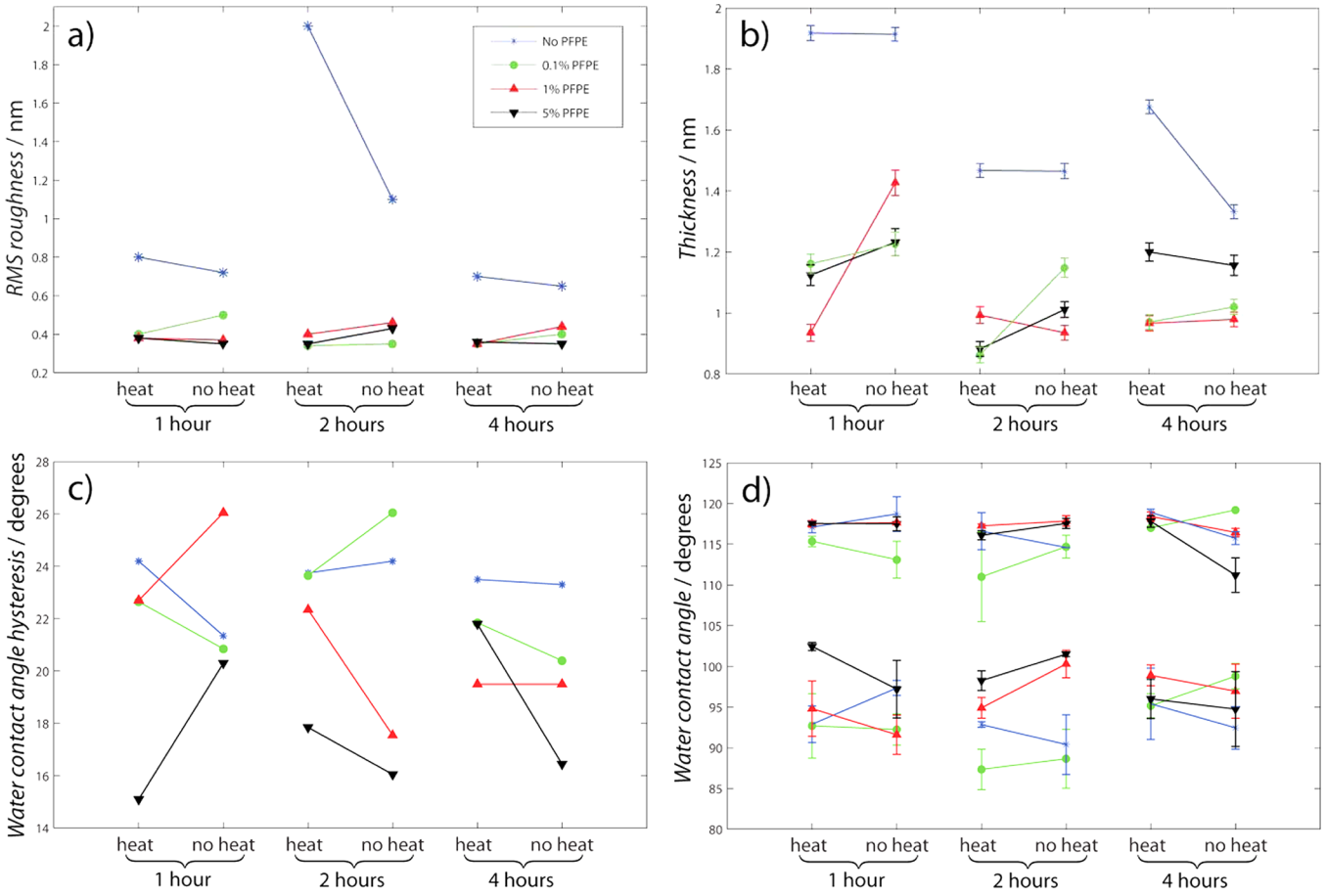

Figure 3. Characterization data for SCA SAMs on silicon dioxide: (a) rms roughness as a function of sample treatment. The untreated silicon dioxide surface rms roughness is 0.35 nm. (b) SAM thickness as measured by ellipsometry. Error from the measurement is shown. (c) Average water contact angle hysteresis of the SAMs. (d) Advancing (top lines) and receding (bottom lines) water contact angles. Standard error bars are shown. Error bars smaller than the symbols cannot be resolved. Heat/no heat refers to 115 °C, 10 s of treatment prior to PFPE deposition. The deposition time is shown on the *x* axis. All samples were held at 115 °C for 10 min after washing. Ellipsometric thicknesses of the pure PFPE films spin coated before SCA deposition are as follows: 5.98 ± 0.025 nm (0.1% PFPE), 60.98 ± 0.16 nm (1% PFPE), and 345.24 ± 5.36 nm (5% PFPE).

at 0.3 Hz. The rms roughness was calculated using Gwyddion software over the qualitatively smoothest 4 μm × 4 μm areas within a 10 μm × 10 μm z-sensor image after removing scars, median height matching, and removing the polynomial background. Contact angle analysis was performed using a Ramé-Hart model 500-F1 advanced goniometer with DropImage Advanced software using DI water. Five μL droplets were used to evaluate the advancing angle; 2 μL of the droplet was retracted to evaluate the receding angle. XPS was conducted (model SSX-100, Surface Science, Inc.) from 0 to 800 eV with a monochromatic Al Kα source with a 1 mm spot size and a 150 eV pass energy. Scanning electron microscope (SEM) (Zeiss EVO) images were taken at an accelerating voltage of 1 kV with a working distance of 3.7 mm normal to the substrate surface.

RESULTS AND DISCUSSION

Monolayer Characterization. Smooth monolayers of SCA without aggregates were produced when deposition through the barrier layer was employed (Figure 2b,e). To verify that the PFPE was removed completely after washing, XPS survey scans of the O 1s peak were recorded from samples and controls, as seen in Figure 2c. The significant separation (~3 eV) between control peaks ("PFPE only", "SAM only") and the precise matching of peak positions for the PFPE/SAM samples to the SAM-only sample illustrate that the washing procedure employed was enough to overcome the hydrogen bonding between the PFPE and the surface[16] and completely remove the barrier. It is expected that PFPE hydrogen bonding with surface silanols or physisorbed water does not prevent SCA molecules from attaching to the surface because the SCA also forms hydrogen bonds with these species, ultimately hydrolyzing and forming permanent, covalent bonds to the surface. The samples selected for XPS analysis were the most likely to contain residual PFPE. A lack of charge-compensation hardware prevented a more detailed comparison of high-resolution peak positions.

Tapping-mode AFM clearly shows agglomerates on the surface when no barrier was employed (Figure 2a) whereas the use of 5% PFPE (Figure 2b) dramatically reduces the average roughness. Figure 3a highlights this roughness improvement showing a decrease by a factor of 2 when employing a PFPE barrier. The large differences in roughness seen for the control samples in Figure 3a ("No PFPE") are primarily due to the high lateral spatial resolution of the AFM technique that is sensitive to local topography. Our conclusions about the roughness are corroborated by the more macroscopic trends gained by ellipsometry and contact angle analysis.

Half of the samples were heated to allow direct comparison between excess surface water (untreated samples) and a few layers of tightly bound surface water (heat-treated samples). The 115 °C treatment should not cause the significant condensation of surface silanols or the removal of tightly

dx.doi.org/10.1021/la303377w | *Langmuir* XXXX, XXX, XXX−XXX

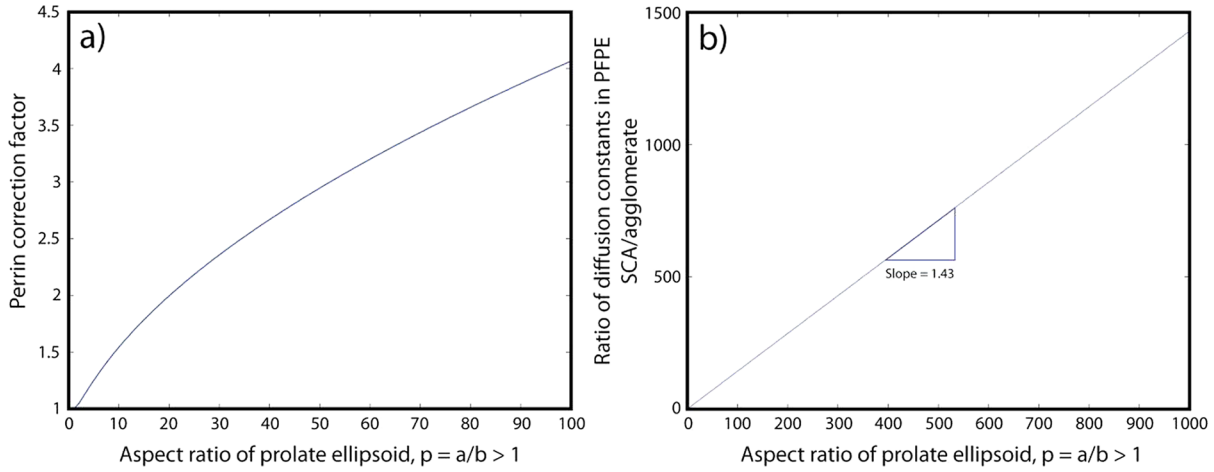

Figure 4. (a) Perrin correction factors for prolate ellipsoids of varying aspect ratio, p. (b) Ratio of translational diffusion constants in PFPE, SCA/agglomerate, for the SCA chemistry employed in this investigation. The selectivity of the barrier is constant for all agglomerate radii, as seen by a constant slope of 1.43.[24] This analysis assumes a linear relationship between aggregate molecular weight and density.

bound water; some physisorbed water is expected to desorb.[17] The rms roughness and contact angle data in Figure 3a,b do not show significant trends with this dehydration, indicating that either the amount of water removed is small or the strongly bound water proximal to the substrate is the most critical in terms of forming a SAM.

Ellipsometry was used to determine SAM thicknesses (Figure 3b). Because ellipsometry provides an average thickness over the projected beam area (~1.5 mm spot diameter), the measurement inherently includes agglomerates. It is clear that the control sample SAMs are thicker than those with barrier layers, but this additional thickness is attributable to the presence of agglomerates. Agglomerates in the control samples are also identified by the increased rms roughness observed by AFM.

The water contact angle data after the removal of the barrier layer are consistent with the high contact angles reported for the particular perfluorinated SCA species on the surface (~115°).[18] The advancing contact angles are also quite similar for the samples without barrier layers, indicating in both cases that the densely packed trifluoro moieties extend outward from the substrate (Figure 3d). The contact angle hysteresis was reduced significantly by using the 5% PFPE barrier under all deposition conditions relative to the surfaces prepared without a barrier layer. This is in agreement with the conclusions from AFM and ellipsometry that the control samples exhibit more heterogeneous surface morphologies through the formation of agglomerates (Figure 3c). It appears that in general, from the water contact angle and water contact angle hysteresis data, the 5% PFPE (thickest barrier) produced the highest-quality films of those evaluated. These data suggest that employing an even thicker PFPE film than we used (>345 nm) may yield even more favorable results.

Surface roughness is known to influence contact angle hysteresis significantly. Johnson and Dettre describe the idealized effect of roughness on hysteresis relative to a perfectly smooth surface.[19] It is readily seen that the advancing and receding angles diverge quickly with relatively small increases in roughness. Although their calculations are based on an idealization, our PFPE-treated surface is relatively smooth (0.4 nm rms) and is expected to be well within the range described by Johnson and Dettre. Quere[20] also cites Johnson and Dettre's work on roughened wax, which indicates using experimental data that the contact angle hysteresis increases significantly as one transitions from a smooth to a rough surface, and decreases substantially upon reaching the Cassie state. Although the observed discontinuity in contact angle hysteresis over large changes in surface roughness is not fully understood, increases in hysteresis of 10° or more for relatively small changes in roughness in the Wenzel state are seen to be plausible.

Diffusion Analysis. It is hypothesized that the separation of agglomerates from individual molecules during diffusion through the PFPE barrier is the primary mechanism for forming smooth SAMs. The present experimental work has identified barrier layer and substrate conditions that result in highly functionalized, smooth SCA monolayers, but qualitative observations indicate that thicker barrier layers appear to yield improved results. Therefore, an optimum barrier layer thickness has not been determined for these specific conditions. To understand how the properties of the barrier layer might affect the process of separating individual molecules from agglomerates, a basic evaluation of the system from a diffusional vantage is employed.[21]

The translational diffusion coefficient, D_t, is described by the Einstein−Stokes equation

$$D_t = \frac{k_b T}{f_t}$$

where the k_b is Boltzmann's constant, T is the temperature, and f_t is the translational friction coefficient defined by the viscosity of the medium, η_0, and the molecular hydrodynamic radius, R_H:

$$f_t = 6\pi\eta_0 R_H$$

Becauase the molecular hydrodynamic radius accounts for the specific geometry of the molecule, Perrin's formulas[21,22] are employed (Figure 4a):

$$R_H = R_{sphere}\frac{\sqrt{p^2 - 1}}{p^{1/3}\ln(p + \sqrt{p^2 - 1})}$$

The molecular aspect ratio

dx.doi.org/10.1021/la303377w | Langmuir XXXX, XXX, XXX−XXX

$$p = \frac{a}{b} > 1$$

allows an approximation of a linear SCA molecule by a prolate ellipsoid, where a and b are two of the semiprincipal axes, such that a third dimension $c = b$. Substituting the radius of a sphere,

$$R_{\text{sphere}} = \left(\frac{3V}{4\pi}\right)^{1/3}$$

R_H can be written in terms of the molecular volume, V,

$$R_H = \left(\frac{3V}{4\pi}\right)^{1/3} \frac{\sqrt{p^2 - 1}}{p^{1/3} \ln(p + \sqrt{p^2 - 1})}$$

and rewritten, substituting for molecular volume

$$V = \frac{M_w}{\rho N_A}$$

$$R_H = \left(\frac{3\frac{M_w}{\rho N_A}}{4\pi}\right)^{1/3} \frac{\sqrt{p^2 - 1}}{p^{1/3} \ln(p + \sqrt{p^2 - 1})}$$

where the molecular volume is given in terms of the molecular weight, M_w, density, ρ,[23] and Avogadro's number, N_A.

The ratio of diffusion times of individual SCA molecules to those of agglomerates determines the selectivity of the barrier and thus the smoothness of the resulting SAM. Because the diffusion constants are determined by the temperature, medium viscosity, SCA/agglomerate molecular weight, SCA/agglomerate density, and aspect ratio, the two diffusivities can be expressed as

$$D_{t,\text{SCA}} \propto \frac{T\rho_{\text{sca}}^{1/3}}{\eta_{o,\text{medium}} M_{w,\text{SCA}}^{1/3}} \frac{p^{1/3} \ln(p + \sqrt{p^2 - 1})}{\sqrt{p^2 - 1}}$$

$$D_{t,\text{agglom}} \propto \frac{T\rho_{\text{agglom}}^{1/3}}{\eta_{o,\text{medium}} M_{w,\text{agglom}}^{1/3}}$$

where agglomerates are assumed to be spherical such that the quantity p applies only to the SCA molecule. The selectivity, namely, the ratio between these diffusion constants, then becomes

$$\frac{D_{t,\text{SCA}}}{D_{t,\text{agglom}}} = \left(\frac{\rho_{\text{SCA}}}{\rho_{\text{agglom}}} \frac{M_{w,\text{agglom}}}{M_{w,\text{SCA}}}\right)^{1/3} \frac{p^{1/3} \ln(p + \sqrt{p^2 - 1})}{\sqrt{p^2 - 1}}$$

Although this relation could be expressed as a ratio of hydrodynamic radii, it is more accurate to account for the fact that the agglomerate density may not scale linearly with density because of disordered molecular packing. If the molecular packing disorder increases with increasing agglomerate molecular weight, then the selectivity of the barrier layer increases nonlinearly.

Our basic calculations predict that the majority of SCA diffusion through submicrometer PFPE barriers occurs within 2000 s.[24] For deposition times on this order, submicrometer PFPE barrier thicknesses have only a minor effect on the final surface SCA concentration. However, PFPE provides a time delay for agglomerates relative to individual SCA molecules diffusing to the surface. This creates a processing window for functionalizing a surface without significant interference from agglomerates. The barrier layer viscosity does not play a role, but rather the physical properties of the SCA and its agglomerates are responsible for the barrier selectivity. Although it is beyond the scope of this article to comment on the diffusional processes themselves, a void-hopping mechanism has been proposed from computational studies of amorphous polymers.[25]

Generalized Barrier Layer Selection. Although the results for the formation of a monolayer on silicon dioxide using a PFPE barrier layer have been described, other barrier layer materials may be more suited for different surfaces and SCA chemistries. For example, certain classes of SCAs are required to modify nonsiliceous substrates such as carbonates and metal oxides.[26] In some cases, such as for perfluorinated SCAs deposited on silicon dioxide with a silicone oil barrier layer, the surface energy of the silicon dioxide changes drastically as SCA is deposited, ultimately causing the barrier layer to dewet. In the following text, we list the general requirements for the selection of suitable barrier layers for the formation of smooth, aggregate-free SAMs.

(1) Ability to form smooth films on the substrate consistently. In this work, we employed a dilute, low-surface-energy polymer solution that did not dewet from a silicon dioxide surface upon spin coating.
(2) Sufficient solubility of the SCA in the barrier material to permit diffusion to the substrate surface within the deposition time frame. We chose an SCA with a highly fluorinated R group in combination with a liquid PFPE barrier.
(3) Complete removal of the barrier material after SCA deposition without damaging the SAM. A good solvent was used to wash away the PFPE after deposition as verified by XPS. Because PFPE interacts with the surface through relatively weak hydrogen bonds, it is reasonable to expect the removal of all residue after thorough washing.
(4) Ability of the barrier layer to prevent water evaporation from the sample surface. Because it is known that a constant water concentration at the substrate surface improves SAM reproducibility,[7] PFPE is a logical choice because it has been observed to possess excellent resistance to water diffusion.[27]
(5) Chemical inertness of the barrier with respect to the SCA. If the barrier reacts with the SCA, then it is much less likely that a sufficient number of SCA molecules will reach the substrate surface before agglomerates arrive.

Although planar substrates may be ideal for creating uniform barrier layers across a wafer surface, applying a barrier layer by spin coating may not be appropriate for patterned substrates with high-aspect-ratio features or significant relief, commonly found in nanoimprint stamping. As the data indicate (Figure 3), for the PFPE barrier layer thicknesses and deposition times employed there is a dependence of SAM properties on the barrier thickness. Therefore, it is necessary to apply the most uniform thickness barrier layer possible. Although the differences in barrier thickness would depend on the exact stamp geometry, other deposition methods designed for coating high-aspect-ratio structures, such as spray coating, have been implemented successfully with photoresist solutions[28] and would be applicable to complex surface structures. The wettability of the substrate by the barrier would influence its conformity and thus the uniformity of the resulting SAM. In the

dx.doi.org/10.1021/la303377w | Langmuir XXXX, XXX, XXX−XXX

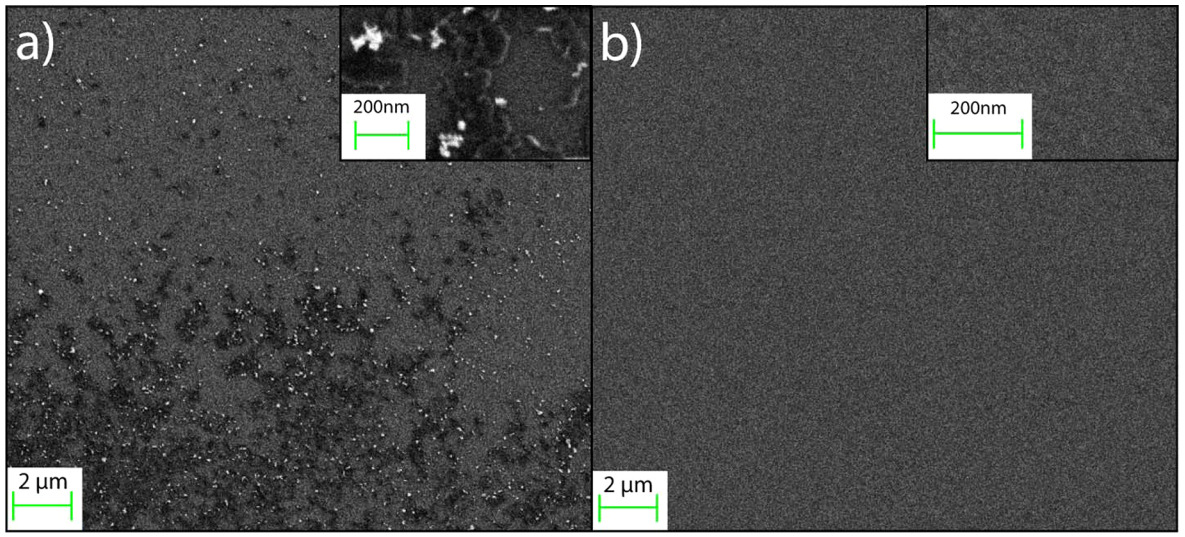

Figure 5. (a) SEM images of SCA deposited on silicon dioxide without any barrier layer. Darker features are suspected to be electron-transparent agglomerates with planar geometry whereas the white features are suspected to be more spherical agglomerates that experience charging under the beam. (b) SCA deposited on silicon dioxide using a 1% solution of silicone oil in heptane. The silicone oil layer was measured to be 52 nm thick by ellipsometry. SCA was deposited for 1 h on both samples. Higher-magnification insets are included.

case of PFPE on silicon dioxide, both perfluorooctane and Fomblin Y exhibit a nearly zero degree water contact angle because of their low surface energies. Although it is beyond the scope of this article, solid, highly conformal barrier layers could be applied in a manner similar to the techniques used in parylene deposition.

Alternate Barrier Layer Materials. In addition to PFPE, we have found that silicone oil in heptane is an acceptable all-purpose barrier layer on silicon dioxide in that it dissolves many silane coupling agents (unlike PFPE) but is disadvantageous because thicker layers can dewet over time. In addition, residual oil is difficult to remove,[29] and when small samples are used (<1 cm^2), significant edge bead formation occurs. For the same SCA, it can be seen from SEM images in Figure 5 that silicone oil barriers can also remove SCA agglomerates effectively. Upon sample inspection after SCA deposition, the silicone oil was observed to dewet as the SCA SAM lowered the substrate's surface energy below that of the silicone oil. Despite dewetting, the silicone oil was effective at preventing agglomerates from adhering to the surface. PFPE is an ideal barrier material for fluorinated SCAs on silicon dioxide because it resists dewetting, forms stable films without a significant edge bead, and can be removed completely. For nonfluorinated SCAs, silicone oil may well be preferable to PFPE as poor solubility becomes problematic. In contrast, heavy mineral oil (Sigma-Aldrich, Inc.) in heptane was observed to be a poor barrier layer on silicon dioxide because of its inherent tendency to dewet upon spin coating, stemming from its inability to entangle with itself[30] or any adsorbed species.[31]

CONCLUSIONS

We have presented a general technique for depositing smooth, aggregate-free SCA SAMs on silicon dioxide through the use of a barrier layer to limit agglomerates from reaching the surface. PFPE barriers have been shown to facilitate the formation of perfluorinated SAMs possessing reduced contact angle hysteresis and reduced surface roughness while maintaining high contact angles while affording complete removal of the barrier. A generalized set of guidelines have been described for barrier material selection. Depending on the application and desired surface chemistry, alternate barrier layer materials such as silicone oil may be more suitable than PFPE. Such a technique is applicable to those desiring chemical functionality, monolayer coverage, smooth surface morphology, reproducible coating properties, and a facile technique requiring only commercially available materials.

ASSOCIATED CONTENT

Supporting Information

SAM density and diffusion analysis. This material is available free of charge via the Internet at http://pubs.acs.org.

AUTHOR INFORMATION

Corresponding Author

*Telephone: 1-617-495-4469. E-mail: rdiebold@seas.harvard.edu.

Notes

The authors declare no competing financial interest.

ACKNOWLEDGMENTS

We thank Professors Edward J. Kramer, Craig J. Hawker, and Michael J. Gordon for many helpful suggestions, Shanying Cui for assistance with XPS measurements, Samuel Shian for assistance with the SEM, and the Whitesides group at Harvard for the use of the contact angle apparatus. This work was performed in part at Harvard University's Center for Nanoscale Systems, a member of the National Nanotechnology Infrastructure Network, which is supported by the National Science Foundation under NSF award no. ECS-0335765 and supported primarily by the MRSEC program of the National Science Foundation under award no. DMR-0820484.

REFERENCES

(1) Plueddemann, E. P. *Silane Coupling Agents*, 2nd ed.; Springer: New York, 1982; p 235.

(2) Sun, Y.; Zhang, Z.; Wong, C. P. Study on mono-dispersed nano-size silica by surface modification for underfill applications. *J. Colloid Interface Sci.* **2005**, *292*, 436−444.

(3) Srinivasan, U.; Houston, M. R.; Howe, R. T.; Maboudian, R. Alkyltrichlorosilane-based self-assembled monolayer films for stiction reduction in silicon micromachines. *J. Micromech. Syst.* **1998**, *7*, 252−260.
(4) Zhuang, Y. X.; Hansen, O.; Knieling, T.; Wang, C.; Rombach, P.; Lang, W.; Benecke, W.; Kehlenbeck, M.; Koblitz, J. Vapor-phase self-assembled monolayers for anti-stiction applications in MEMS. *J. Micromech. Syst.* **2007**, *16*, 1451−1460.
(5) Aswal, D. K.; Lenfant, S.; Guerin, D.; Yakhmi, J. V.; Vuillaume, D. Self assembled monolayers on silicon for molecular electronics. *Anal. Chim. Acta* **2006**, *568*, 84−108.
(6) Gnanappa, A. K.; O'Murchu, C.; Slattery, O.; Peters, F.; O'Hara, T.; Aszalós-Kiss, B.; Tofail, S. A. M. Improved aging performance of vapor phase deposited hydrophobic self-assembled monolayers. *Appl. Surf. Sci.* **2011**, *257*, 4331−4338.
(7) Ulman, A. Formation and structure of self-assembled monolayers. *Chem. Rev.* **1996**, *96*, 1533−1554.
(8) Jung, G. Y.; Li, Z.; Wu, W.; Chen, Y.; Olynick, D. L.; Wang, S. Y.; Tong, W. M.; Williams, R. S. Vapor-phase self-assembled monolayer for improved mold release in nanoimprint lithography. *Langmuir* **2005**, *21*, 1158−1161.
(9) Silberzan, P.; Leger, L.; Ausserre, D.; Benattar, J. J. Silanation of silica surfaces. A new method of constructing pure or mixed monolayers. *Langmuir* **1991**, *7*, 1647−1651.
(10) Benkoski, J. J.; Kramer, E. J.; Yim, H.; Kent, M. S.; Hall, J. The effects of network structure on the resistance of silane coupling agent layers to water-assisted crack growth. *Langmuir* **2004**, *20*, 3246−3258.
(11) Iler, R. K. *The Chemistry of Silica: Solubility, Polymerization, Colloid and Surface Properties, and Biochemistry*. Wiley: New York, 1979.
(12) Hair, M. L.; Hertl, W. Reactions of chlorosilanes with silica surfaces. *J. Phys. Chem.* **1969**, *73*, 2372−2378.
(13) Allara, D. L.; Parikh, A. N.; Rondelez, F. Evidence for a unique chain organization in long chain silane monolayers deposited on two widely different solid substrates. *Langmuir* **1995**, *11*, 2357−2360.
(14) Genzer, J.; Efimenko, K.; Fischer, D. A. Molecular orientation and grafting density in semifluorinated self-assembled monolayers of mono-, di-, and trichloro silanes on silica substrates. *Langmuir* **2002**, *18*, 9307−9311.
(15) Brzoska, J. B.; Azouz, I. B.; Rondelez, F. Silanization of solid substrates: a step toward reproducibility. *Langmuir* **1994**, *10*, 4367−4373.
(16) Zhao, Z.; Bhushan, B.; Kajdas, C. Tribological performance of PFPE and X-1P lubricants at head−disk interface. Part II. Mechanisms. *Tribol. Lett.* **1999**, *6*, 141−148.
(17) Iler, R. K. *The Chemistry of Silica Solubility, Polymerization, Colloid and Surface Properties, and Biochemistry*; Wiley: New York, 1979.
(18) Schift, H.; Saxer, S.; Park, S.; Padeste, C.; Pieles, U.; Gobrecht, J. Controlled co-evaporation of silanes for nanoimprint stamps. *Nanotechnology* **2005**, *16*, S171−S175.
(19) Johnson, R. E.; Dettre, R. H. Contact Angle Hysteresis - I. Study of an Idealized Rough Surface. In *Contact Angle, Wettability, and Adhesion*; Fowkes, F. M., Ed.; American Chemical Society: Washington, DC, 1964; Vol. *43*, pp 112−135.
(20) Quere, D. Rough ideas on wetting. *Physica A* **2002**, *313*, 32−46.
(21) Hansen, S. Translational friction coefficients for cylinders of arbitrary axial ratios estimated by Monte Carlo simulation. *J. Chem. Phys.* **2004**, *121*, 9111−9115.
(22) Perrin, F. Mouvement brownien d'un ellipsoide (II). Rotation libre et depolarisation des fluorescences. Translation et diffusion de molecules ellipsoidales. *J. Phys. Radium* **1936**, *7*, 1−11.
(23) (Tridecafluoro-1,1,2,2-tetrahydrooctyl)trichlorosilane MSDS. Gelest: 2008.
(24) See Supporting Information.
(25) Muller-Plathe, F. Diffusion of penetrants in amorphous polymers: a molecular dynamics study. *J. Chem. Phys.* **1991**, *94*, 3192−3199.
(26) Arkles, B. *Silane Coupling Agents: Connecting Across Boundaries*; Gelest: Morrisville, PA, 2006; p 18.
(27) Porter, J. J.; Klassen, J. K.; Nathanson, G. M. Penetration of water vapor through perfluorinated polyether films on concentrated sulfuric acid. *Langmuir* **1996**, *12*, 5448−5450.
(28) Cooper, K. A.; Hamel, C.; Whitney, B.; Weilermann, K.; Kramer, K. J.; Zhao, Y.; Gentile, H. *Conformal Photoresist Coatings for High Aspect Ratio Features*; Proceedings of the International Wafter Level Packaging Conference; Suss MicroTec, 2007.
(29) Papirer, E. *Adsorption on Silica Surfaces*; Marcel Dekker: New York, 2000.
(30) Spangler, L. L.; Torkelson, J. M.; Royal, J. S. Influence of solvent and molecular weight on thickness and surface topography of spin-coated polymer films. *Polym. Eng. Sci.* **1990**, *30*, 644−653.
(31) Yerushalmi-Rozen, R.; Klein, J.; Fetters, L. J. Suppression of rupture in thin, nonwetting liquid films. *Science* **1994**, *263*, 793−795.